International Journal of Pharmaceutics 418 (2011) 179–186

Contents lists available at ScienceDirect

International Journal of Pharmaceutics

journal homepage: www.elsevier.com/locate/ijpharm

Interplay between molecular conformation and intermolecular interactions in conformational polymorphism: A molecular perspective from electronic calculations of tolfenamic acid

Alessandra Mattei, Tonglei Li*

Department of Pharmaceutical Sciences, University of Kentucky, Lexington, KY 40536, United States

ARTICLE INFO

Article history:
Received 23 November 2010
Received in revised form 17 April 2011
Accepted 26 April 2011
Available online 5 May 2011

Keywords:
Polymorphism
Molecular conformation
Intermolecular interactions
Conceptual density functional calculations

ABSTRACT

Tolfenamic acid exhibits conformational polymorphism. The molecules in its two commonly occurred crystal structures form similar hydrogen-bonded dimers but differ in conformation. The conformational variance was analyzed by electronic calculation methods with the aim to unravel intrinsic connection between the conformational flexibility and intermolecular interactions in the polymorphs. The study was conducted mainly by conceptual density functional theory (DFT) and natural bond orbital (NBO) analysis. It is found that the conformational polymorphism is resulted from the energy competition between intramolecular π-conjugation and intermolecular hydrogen bonding. By adapting conformation that departs from being the most energetically stable, tolfenamic acid molecules can strengthen the intermolecular hydrogen-bonding interactions in the crystals. The study illustrates how the molecule's electronic properties are influenced by conformational variation and, inherently, how the intermolecular interactions become regulated. Moreover, understanding molecular interaction and crystal packing necessitates electronic structure calculation and analysis, which can be further facilitated by utilizing DFT and NBO concepts.

© 2011 Elsevier B.V. All rights reserved.

1. Introduction

Organic molecules, including most of drug substances, are inclined to polymorphic formation in the solid state (Byrn et al., 1999). Polymorph screening is increasingly assisted by computational techniques to identify all possible physical forms and further to select the most suitable polymorph for drug development (Brittain, 2009; Price, 2009). It is well known that formation of distinct crystal structures of the same molecule is greatly influenced by thermodynamic and kinetic factors, including type of solvents (Threlfall, 2000; Parmar et al., 2007; Long et al., 2008) and use of additives (Addadi et al., 1985; Davey et al., 1997; Weissbuch et al., 2003; Lee et al., 2008). Little is known, nonetheless, regarding the fundamental mechanism of the self-assembling process of crystallization under various growth conditions. Still, high-performance computation has and will play an important role in advancing the field of organic crystals to permit examination of molecular events and interactions of crystal packing.

In conformational polymorphs of organic molecules, molecular conformation and intermolecular interaction are energetically intertwined. A specific crystal structure reflects a delicate energy balance or compromise between intermolecular forces that are responsible for the structural arrangements and molecular conformations that are adopted by molecules in the crystal (Etter, 1990). It is known that the energy difference among possible polymorphs of an organic molecule can be as low as 2 kJ/mol, or even lower (Hollingsworth, 2002; Nangia, 2008; Yu, 2010). Thus, a small conformational energy change can result in a totally different crystal packing motif (Long and Li, 2009). Conversely, a particular intermolecular interaction arrangement, for instance, imposed by some specific solvent environment, may call for a unique conformation in the resultant crystal. Hydrogen-bonding is undoubtedly the most critical force in holding organic molecules in the solid state, not only due to its strength but also to its highly directional nature (Steiner, 2002; Desiraju, 2007). Understanding of the energy relationship between a molecule's conformation and its intermolecular interactions is imperative to the field of crystal growth and the utmost aim of rationalizing polymorph formation and predicting crystal structures.

Conceptual density functional theory (DFT) has been of considerable interest for studying chemical reactivity and molecular interaction (Parr and Yang, 1989; Ayers and Levy, 2000; Geerlings et al., 2003). By calculating and examining how the electronic

* Corresponding author at: Room 375, Biological/Pharmaceutical Complex, University of Kentucky, 789 South Limestone, Lexington, KY 40536-0596, United States. Tel.: +1 859 257 1472; fax: +1 859 257 7585.
E-mail address: tonglei@uky.edu (T. Li).

0378-5173/$ – see front matter © 2011 Elsevier B.V. All rights reserved.
doi:10.1016/j.ijpharm.2011.04.062

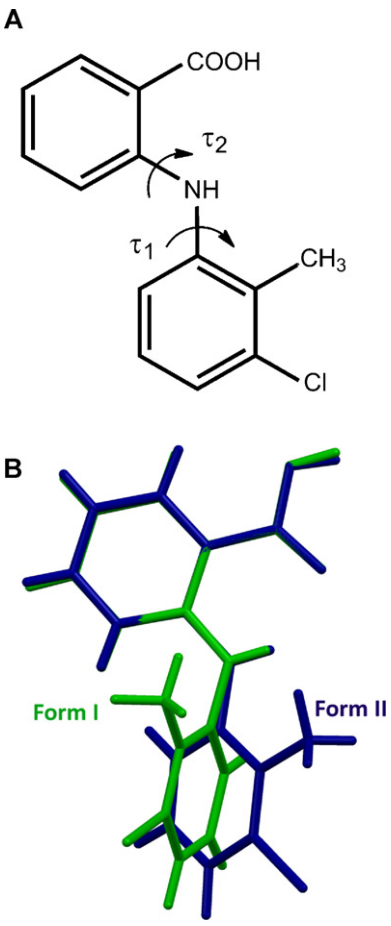

Fig. 1. Molecular structure of TFA (A) and overlay of the two conformers from form I, green; form II, blue (B). Torsion angles, τ_1 and τ_2, are denoted.

structure of a molecular system responds to electronic perturbation (e.g., change of the number of electrons in the system), the intrinsic behavior of the molecule interacting with other systems, physically and chemically, can be characterized. As it bridges the gap between physicochemical properties and underlying structural causes, the theory allows studies of chemical reactivity and molecular interaction from the viewpoint of electron density and its derivatives. The conceptual DFT is being actively developed and embraced for studying chemical reactivity (Huang et al., 2008; Roy and Chattaraj, 2008; Cardenas et al., 2009; Feng et al., 2009; Ugur et al., 2009). A few attempts have been made by our group to characterize intermolecular interactions of organic crystals (Li, 2007; Aubrey-Medendorp et al., 2008; Li et al., 2009), demonstrating great potentials for studying molecular packing.

Herein, we report a study of electronic calculations and DFT analyses of the conformational polymorphism of tolfenamic acid (TFA, Fig. 1A), a nonsteroidal anti-inflammatory drug (NSAID). Two major polymorphs (forms I and II) are routinely encountered, while three new ones were discovered recently by crystallization from polymeric environment (Andersen et al., 1989; Lopez-Mejias et al., 2009). The main difference in the molecular conformation in forms I and II stems from the torsion angle τ_1 (−74.9° and −142.6° in forms I and II, respectively). Similar hydrogen-bonded dimer motifs between neighboring carboxyl groups exist in all of the crystal structures. Previous experimental studies in our group showed that crystallization of form I or II from ethanol depends on the solute concentration (published elsewhere). In brief, it was found that at low supersaturation the metastable form II was obtained, while at high supersaturation form I started to appear. UV absorptivity measurement of the drug in ethanol solutions of various concentrations indicated that solute molecules form more hydrogen-bonded dimers when the concentration increases. Additionally, the intermolecular hydrogen-bonding strength of the two dimer motifs resembled in forms I and II was calculated. The geometry of each dimer was taken directly from the respective crystal structure, underwent constrained optimization with τ_1 and the intermolecular distances between oxygen atoms of the hydrogen-bonded carboxyl groups held constant. The root-mean-square values of atomic coordinates due to the dimer optimization were 0.021 and 0.009 Å of forms I and II, respectively. Intermolecular interaction energies of the optimized cyclic dimers were then calculated in gas phase at two different levels of B3LYP/6-31+G(d,p) and MP2/6-31+G(d,p); the basis set superposition error (BSSE) was also considered by the counterpoise method (Boys and Bernardi, 1970). It was found that the hydrogen-bonding strength of the form I dimer was 3 kJ/mol stronger than that of the form II dimer, while the potential energy of the form I conformer was 3–4 kJ/mol less stable, calculated by DFT and MP2, respectively. Thereby, our hypothesis about the concentration effect on the polymorphic formation is constructed based on the fundamental relationship between molecular conformation and intermolecular interaction. It seems plausible that, during the crystallization process, solute molecules bear a conformation similar to that found in the consequent crystal structure. When the monomer is the predominant solute species, the molecule takes its most stable conformation, which resembles that found in form II. As the concentration increases, hydrogen-bonded dimers become the major species and the molecules have to adjust to a less-energy favorable conformation similar to that in form I but form stronger intermolecular hydrogen bonds. As a result, nucleation of the most stable polymorph (i.e., form I) is warranted. The study in this report provides further support to our hypothesis by utilizing DFT-based concepts and natural bond orbital (NBO) analysis to characterize electronic structures of the molecule and examine how the conformational flexibility impacts the polymorphic formation. In all, our studies point to a critical role by solution conformation that is affected by growth conditions in nucleation and polymorphic formation of organic molecules.

2. Theory and methods

2.1. Theoretical background

Within the framework of conceptual DFT, several electronic concepts have been developed for defining a molecule's interacting capabilities with other molecules (Yang and Parr, 1985; Parr et al., 1999; Geerlings et al., 2003; Morell et al., 2005). Two pertinent functions that are utilized in this work are Fukui function and dual descriptor (the calculation details are given in the next section). The electronic Fukui function, $f(r)$, is defined as the change in electron density, $\rho(r)$, upon the change in the total number of electrons, N, at constant external potential, $v(r)$ (Ayers and Levy, 2000; Parr and Yang, 1984):

$$f(r) = \left(\frac{\partial \rho(r)}{\partial N}\right)_{v(r)} \tag{1}$$

The external potential is defined by nuclei of a given molecular system (both nuclear charges and their positions). Because of the discontinuity of the number of electrons being integers (Ayers, 2008; Perdew et al., 1982), nucleophilic Fukui function, $f^+(r)$, and the electrophilic Fukui function, $f^-(r)$, are introduced as:

$$\begin{aligned} f^+(r) &= \rho^+(r) - \rho^0(r) \approx \rho_{\mathrm{LUMO}}(r) \\ f^-(r) &= \rho^0(r) - \rho^-(r) \approx \rho_{\mathrm{HOMO}}(r) \end{aligned} \tag{2}$$

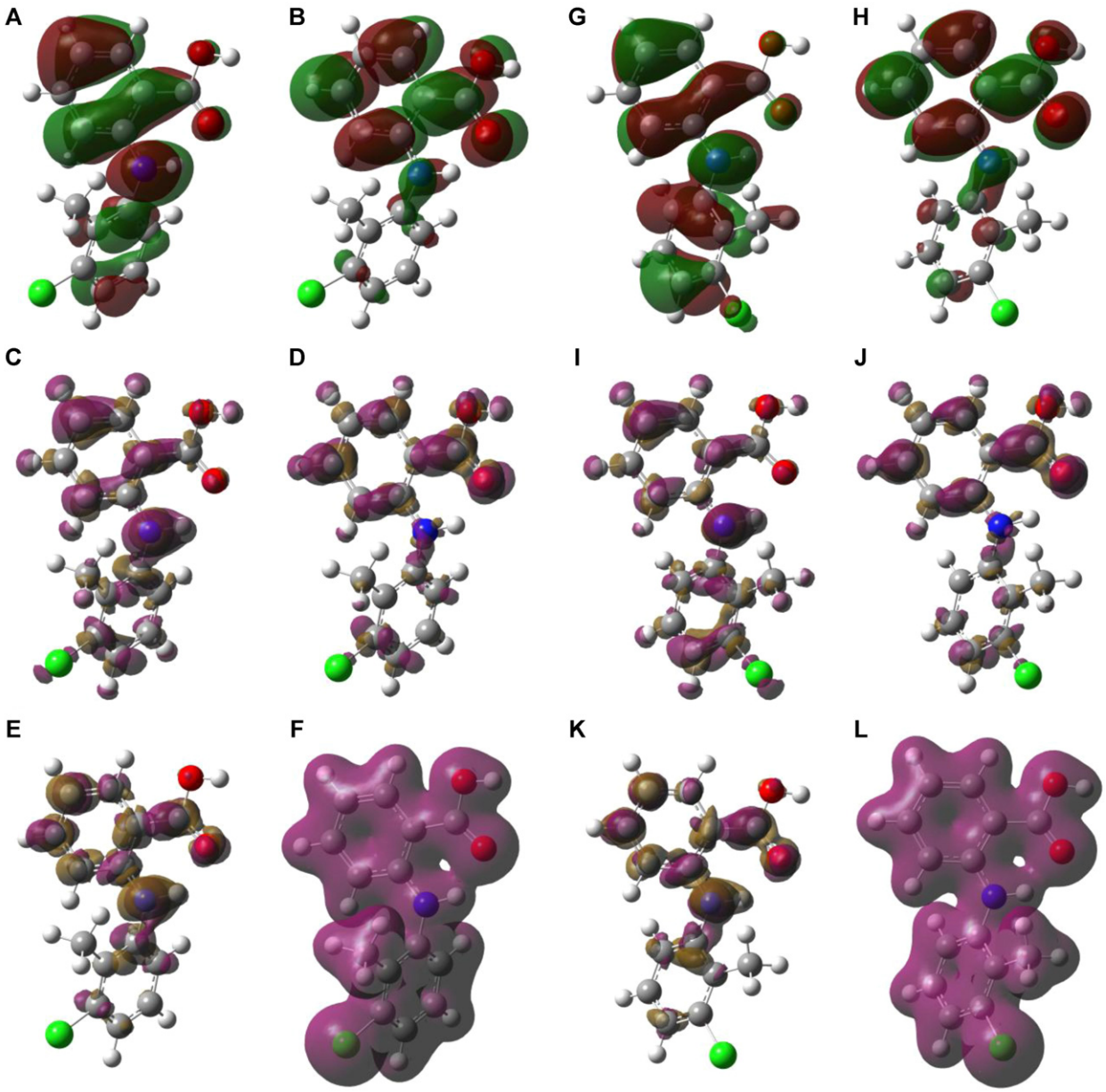

Fig. 2. Highest occupied molecular orbital (A and G), lowest occupied molecular orbital (B and H), electrophilic Fukui function (C and I), nucleophilic Fukui function (D and J), dual descriptor (E and K), and electron density (F and L) isosurfaces of the single molecule taken from forms I and II. The values of isosurfaces are 0.02 a.u. for the frontier orbitals and electron density and 0.002 a.u. for the Fukui functions and dual descriptor, respectively.

In these equations, $\rho^{+}(r)$, $\rho^{-}(r)$, and $\rho^{0}(r)$ represent the electron densities of anionic, cationic, and neutral species of a given molecular system, respectively (Ayers and Levy, 2000). The Fukui functions can be approximated as the electron densities of the frontier orbitals (LUMO, the lowest unoccupied molecular orbital, and HOMO, the highest occupied molecular orbital), because the depletion of electrons generally occurs at the HOMO while the addition of electrons occurs at the LUMO. Examples of these functions of TFA single molecule clearly illustrate the similarity between the HOMO (Fig. 2A and G of forms I and II conformers) and $f^{-}(r)$ (Fig. 2C and I) and between the LUMO (Fig. 2B and H) and $f^{+}(r)$ (Fig. 2D and J), while the electron density (Fig. 2F and L) seems to be just indicative of the shape of the molecule.

Another DFT concept is dual descriptor or second-order Fukui function, $f^{(2)}(r)$ (Morell et al., 2005), which is defined as the second derivative of the electronic density with respect to the number of electrons:

$$f^{(2)}(r) = \left(\frac{\partial^2 \rho(r)}{\partial N^2}\right)_{v(r)} \tag{3}$$

The physical meaning of $f^{(2)}(r)$ is made clear by considering the finite difference approximation (Ayers and Levy, 2000; Ayers et al., 2007):

$$f^{(2)}(r) = f^{+}(r) - f^{-}(r) \approx \rho_{\mathrm{LUMO}}(r) - \rho_{\mathrm{HOMO}}(r) \tag{4}$$

It is shown that $f^{(2)}(r)$ is positive at local regions that prefer to accept electrons or be electrophilic and negative at local regions that prefer to donate electrons or be nucleophilic. Fig. 2E and K depict dual descriptor isosurfaces, illustrating both electrophilic and nucleophilic regions of the conformers in forms I and II, respectively. Because these are local functions, it is chemically more

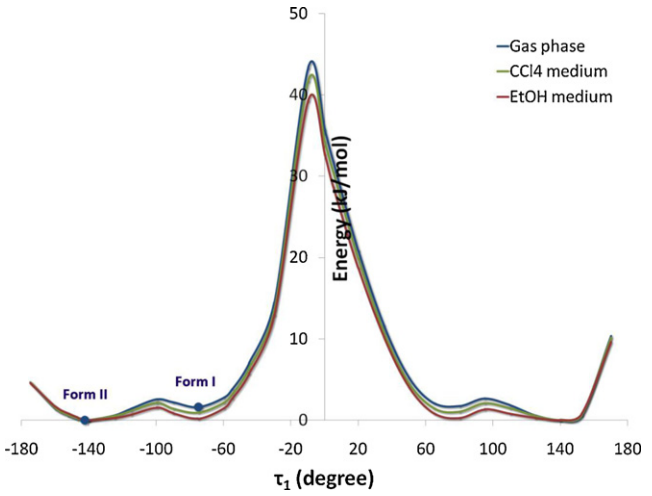

Fig. 3. Conformational energy of TFA single molecule as a function of τ_1 in gas phase, ethanol, and tetrachloromethane solvent media. The torsion angles of forms I and II are marked along the *X*-axis.

convenient to examine nucleophilic or electrophilic centers associated with individual atoms. For this purpose, condensed Fukui functions have been proposed (Yang and Mortier, 1986; Ayers et al., 2002), in an analogy to using atomic charges for partitioning the electron density. The condensed Fukui functions can be calculated as:

$$f_\alpha^+ = q_\alpha^0 - q_\alpha^+ = n_\alpha^+ - n_\alpha^0$$
$$f_\alpha^- = q_\alpha^- - q_\alpha^0 = n_\alpha^0 - n_\alpha^- \quad (5)$$
$$f_\alpha^{(2)} = f_\alpha^+ - f_\alpha^-$$

Here q_α^+, q_α^-, and q_α^0 and n_α^+, n_α^-, and n_α^0 denote the atomic charges and atomic populations on the anionic, cationic, and neutral molecular systems, respectively (Ayers et al., 2002).

2.2. Computational methodology

The conformational flexibility of tolfenamic acid was studied by performing a potential energy scan in gas phase as a function of the torsion angle, τ_1. Single molecules of TFA forms I and II, extracted from their respective crystal structures (Andersen et al., 1989; *R* indices of the respective crystal structures are 5.2% and 2.9%), were fully optimized in order to identify the most stable conformation. The globally energy minimum conformer subsequently was used for scanning τ_1 from −180° to +180° with a step size of 2.5°. At each step, all bond lengths, bond angles, and other torsion angles were allowed to be fully optimized. Energy, electronic structure, and properties of each τ_1-fixed and otherwise fully optimized conformer were then calculated. These quantities were computed in gas phase as well as in solvent media of ethanol and tetrachloromethane, which were modeled using the polarizable continuum model (PCM) within the self-consistent reaction field theory (Barone et al., 1997; Amovilli et al., 1999).

Condensed Fukui functions in gas phase and in solvent media were calculated according to Eq. (5) based on partial atomic charges by NBO analysis (Reed et al., 1988). The NBO charges prove to be robust in electron population analysis (Frenking and Frohlich, 2000). NBO calculation was also used to obtain donor–acceptor stabilization energies by the second-order perturbation theory (Reed et al., 1988; Reed and Weinhold, 1983). The donor–acceptor energy describes quantitatively the electronic bonding–antibonding interaction, providing further intuition about local bonding strengths and intramolecular stability. The calculations were performed by the B3LYP functional (Becke, 1988) with basis sets of 6-311G(d,p) and 6-311++G(d,p) for the structural optimization and conformational analysis, respectively. All DFT calculations were carried out using Gaussian 03 program package (Frisch et al., 2004), while isosurfaces were constructed with GaussView 4.0 (Dennington et al., 2003).

It is worth pointing out that conventional DFT calculation methods cannot fully consider dispersion energy (Kohn et al., 1998; Dobson et al., 2001), which may account for a considerable portion of intermolecular interactions of organic molecules and crystals (Dunitz and Gavezzotti, 2009; Li et al., 2009). Electronic concepts by conceptual DFT, on the other hand, may be better suited for

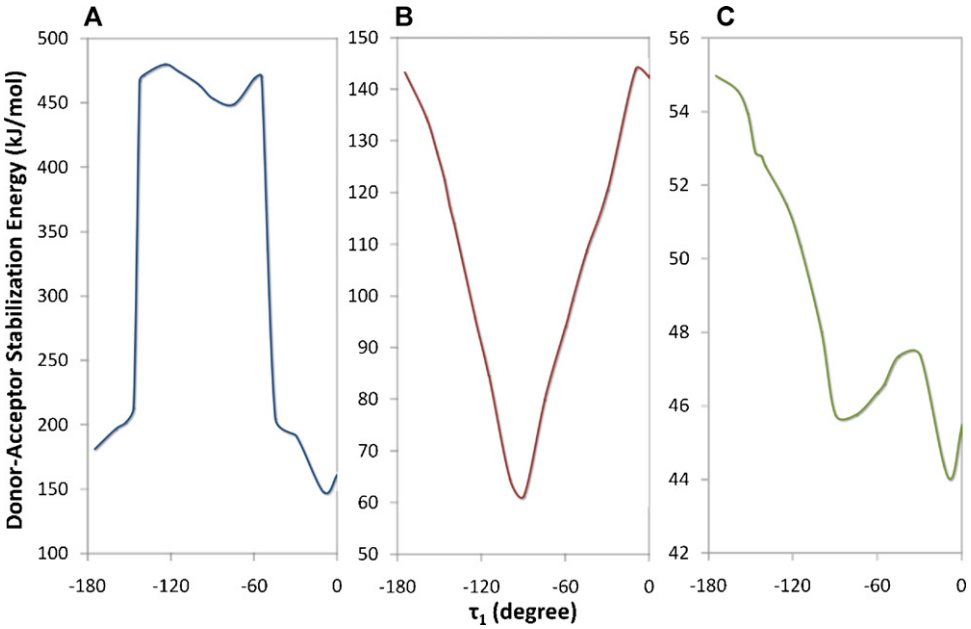

Fig. 4. Donor–acceptor stabilization or bonding–antibonding interaction energies as a function of τ_1 between the nitrogen lone pair and the carboxylated aromatic ring (A), between the nitrogen lone pair and the chlorinated aromatic ring (B), and between the carbonyl oxygen lone pairs and the amino group (C), respectively.

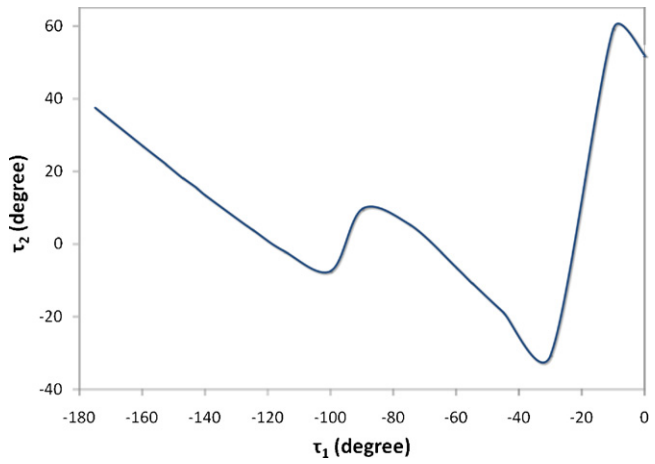

Fig. 5. τ_2 as a function of τ_1 in respective τ_1-fixed conformers that are fully optimized.

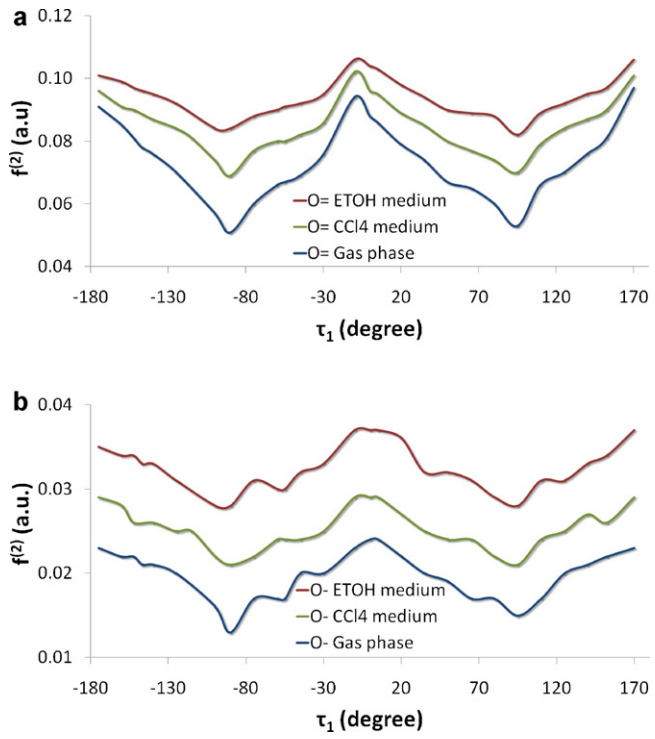

Fig. 6. Condensed dual descriptors of the carbonyl oxygen (a) and hydroxyl oxygen (b) of TFA single molecule as a function of τ_1. The values of each conformation were calculated in gas phase, ethanol, and tetrachloromethane solvent media, respectively.

characterizing molecular interactions. In particular, Fukui function, defined as a second-order derivative of electronic energy, is capable of revealing intermolecular, non-covalent interactions (Li et al., 2009). It is directly related to local polarizability of a molecular system (Ayers, 2007) and, more importantly, is associated with interactions due to partially sharing of electrons (e.g., hydrogen-bonding).

3. Results and discussion

The molecular conformation in the tolfenamic acid polymorphs differs mainly in the torsion angle τ_1 at the chlorinated aromatic ring portion, not in the anthranilic acid moiety (Fig. 1B). The conformational energy of TFA was plotted against τ_1 (Fig. 3). The global energy minimum of the single molecule is located at −142°, which corresponds to the conformer in form II. A shallow minimum at −75° contains the conformer in form I. As the molecules of TFA polymorphs reside closely to the energy minimum regions (within 2 kJ/mol in gas phase as well as in solvent media), the polymorphism of TFA apparently stems from the conformational variance of the molecule itself. In addition, the bonding–antibonding interaction energies were calculated between the lone pair of the amino group and the carboxylated aromatic ring as well as between the lone pair and the chlorinated aromatic ring. Because of the molecule's symmetry around τ_1, only the energies corresponding to negative values of torsion angle, τ_1, are shown in Fig. 4. Of any conformation, the bonding–antibonding interaction energies between the lone pair and the carboxylated aromatic ring (Fig. 4A) are significantly stronger than those between the lone pair and the chlorinated aromatic ring (Fig. 4B). This indicates that the nitrogen atom has a greater tendency to donate electrons to the carboxylated aromatic ring, thus forming a π-conjugated system in the anthranilic portion. Indeed, the chemical bonds calculated by NBO are $sp^{2.48}$ and $sp^{2.70}$ for the N–C in the anthranilic and N–C in the chlorinated phenyl moieties, respectively. Moreover, the form II conformer exhibits higher bonding–antibonding interaction energy values between the nitrogen lone pair and chlorinated aromatic ring than form I (i.e., 117.07 and 79.96 kJ/mol for forms II and I, respectively). As such, the molecular conformation of form II is overall flatter or more conjugated by the two aromatic rings bridged by the amino group ($\tau_1 = -142.6°$ and $\tau_2 = 15.4°$ in form II vs. $\tau_1 = -74.9°$ and $\tau_2 = 5.4°$ in form I). A closer examination of the energy contribution from the π-conjugation as defined by τ_2 (Fig. 4A) reveals that this stabilizing orbital interaction is determinant in conformations when τ_1 is between −142° and −55°, suggesting that the torsion angle, τ_1, must be in this range for the π-conjugation to be retained. The main factor responsible for this behavior is the steric hindrance between the hydrogen at the *meta* position of the carboxylated aromatic ring and the hydrogen or the methyl group at the *ortho* positions of the chlorinated aromatic ring. The steric factor prevents the anthranilic moiety from remaining planar and the extent of non-planarity is illustrated by a systematic variation of τ_2 values as τ_1 changes (Fig. 5). Significant departure from planarity of the anthranilic moiety occurs with τ_1 lying beyond −142° and −55°, in line with the bonding–antibonding interaction energy (Fig. 4). Thus, although τ_1 mainly determines the TFA conformational flexibility, strong cooperativity is observed between neighboring torsion angles, τ_1 and τ_2. More importantly, the nitrogen lone pair delocalization toward the two aromatic rings accounts for the molecule's conformational distribution.

TFA molecule also bears an intramolecular hydrogen bond between the hydrogen-bonding donor amino group and the acceptor carbonyl oxygen. To examine how this feature influences molecular conformation and structural stability, the bonding–antibonding interaction energies between the carbonyl oxygen lone pairs and the amino group are shown as a function of τ_1 (Fig. 4C). The values are 45.77 and 52.80 kJ/mol for forms I and II, respectively. The larger intramolecular hydrogen-bonding contribution in the form II conformer indicates that its anthranilic acid portion is more constrained by the intramolecular hydrogen-bonding, contributing to the coplanarity of the whole molecule. This further implies that TFA molecule is more inclined to adopt a planar conformation; such preference arises primarily from the conjugation or delocalization of the lone pair on the amino group to bridge the two aromatic rings and, in turn, forms a stronger intramolecular hydrogen-bonding.

Intermolecular interaction competes with intramolecular hydrogen-bonding, resulting in variation in conformation. To study the deterministic effect by the molecule's conformation on the intermolecular interaction strength, condensed Fukui functions

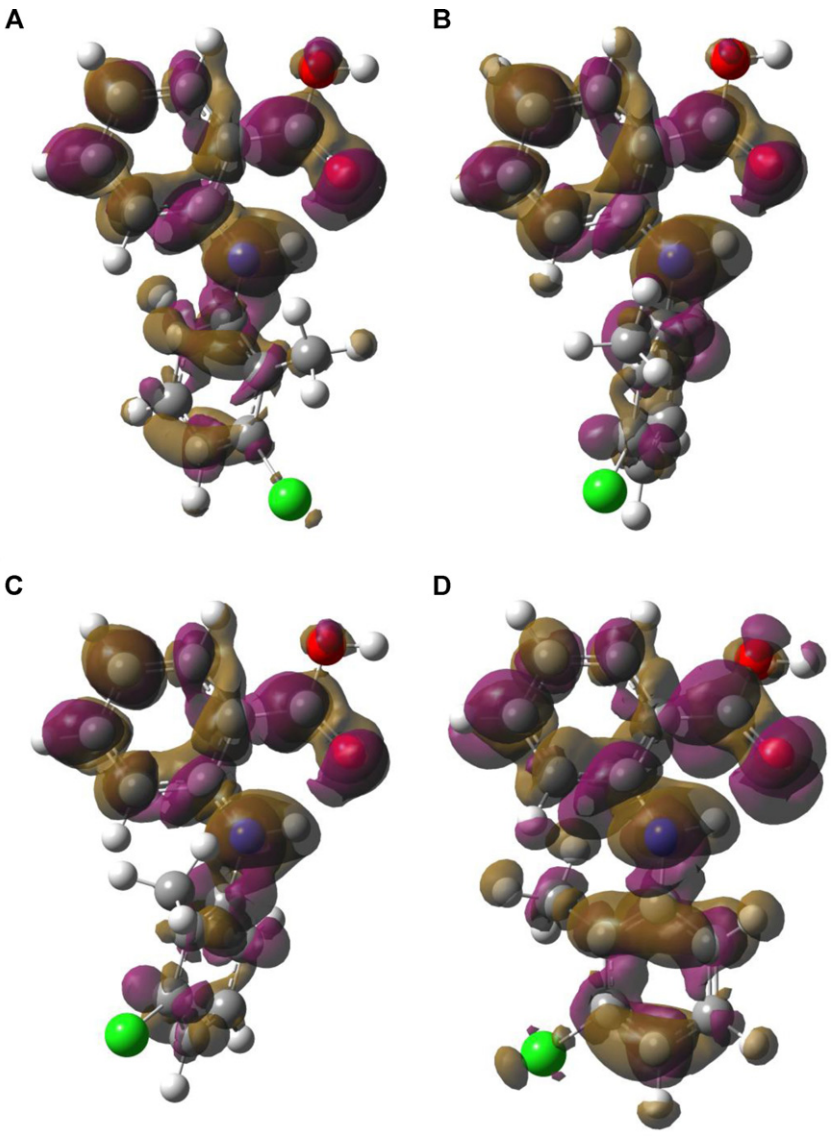

Fig. 7. Dual descriptor isosurfaces (0.001 a.u.) of fully optimized conformers when τ_1 is kept at −142.6° (A), −90° (B), −74.9° (C), or −10° (D). Electrophilic regions are shown in pink and the nucleophilic regions in brown.

were calculated. Dual descriptor magnitudes as a function of the torsion angle, τ_1, were obtained for the carbonyl oxygen and the hydroxyl oxygen atoms (Fig. 6). In gas phase the dual descriptors of the carbonyl oxygen are 0.060 in form I and 0.078 in form II, meaning that the atom in form I is less electrophilic and offers a greater capacity to donate electrons to an electron-deprived hydrogen forming a stronger hydrogen bond (Fig. 6A). Conversely, being part of a π-conjugated system and being further stabilized by an intramolecular hydrogen-bonding, the carbonyl group in form II becomes a relatively poor hydrogen-bonding acceptor. In addition, the carbonyl oxygen has the lowest dual descriptor value (i.e., highest capability to donate its valence electrons) when $\tau_1 = \pm 90°$, a position that completely disrupts the π-conjugation between the amino group and the chlorinated aromatic ring. Dual descriptor isosurfaces further clarify the assessment (Fig. 7). In agreement with the condensed values, a more pronounced nucleophilic region is shown around the carbonyl oxygen of the molecular conformation when $\tau_1 = -90°$ (Fig. 7B). This region thereby contributes considerably to the intermolecular interactions. In comparison, a larger distribution of the electrophilic nature of dual descriptor encloses the hydrogen-bonding moiety of the conformation when $\tau_1 = -10°$, showing the lowest susceptibility to electron donation (Fig. 7D). The two conformers in forms I and II display dual descriptors in-between ($\tau_1 = -142.6°$ or $-74.9°$; Fig. 7A and C). Therefore, the conformational flexibility around τ_1, the π-conjugation defined by τ_2 (i.e., the planarity of the anthranilic moiety), and the electronic distribution determines in cohort the most favorable conformers in order to strengthen intermolecular contacts.

To further understand solvent effect on the intermolecular hydrogen-bonding, condensed Fukui functions were calculated in two solvent media of different polarity, namely, ethanol and tetrachloromethane. As expected, the dual descriptor values of the carbonyl oxygen increase in the solution phase as compared with the gas phase (Fig. 6A), indicating that its electron-donating capability becomes weakened upon solvation, specifically in a polar medium. Similarly, the dual descriptors of the hydroxyl oxygen in gas phase are 0.017 in form I and 0.021 in form II and increase by 0.5% and 1% when computed in tetrachloromethane and in ethanol, respectively (Fig. 6B). Note that the solvent effect was evaluated implicitly. Nonetheless, the general conclusion is held regarding the intrinsic connection between the molecule's conformation and intermolecular hydrogen-bonding strength.

The interplay between intra- and intermolecular interactions may play the crucial role in the concentration effect on the polymorphic formation, as observed in ethanol. At low solution concentration, the monomer is the predominant solute species and takes a conformation that leans toward being planar, leading to the occurrence of form II. Upon concentration increase, solute contacts get strengthened and hydrogen-bonded dimers become dominant as main solute species. The need for stronger intermolecular interactions (because of chemical potential) likely induces a torsional strain in the molecule and favors a conformation where the delocalization of electrons is reduced. When considering the conformational variation from the flatter conformer in form II to the twisted conformer in form I, the torsional strain raises the energy barrier to about 2 kJ/mol (Fig. 3 as $\tau_1 = -74.9^\circ$ in form I and -142.6° in form II). The energy penalty for the rearrangement of molecular conformation and for the consequent loss of π-conjugation is recovered from gaining a stronger hydrogen-bonding (*ca.* 3 kJ/mol calculated by quantum mechanics). This justifies the resultant crystallization of form I. It is thereby reasonable to believe that a unique molecular conformation is a compromise in energy between π-conjugation and intermolecular interaction strength regulated by growth conditions.

It is worth mentioning that the conformational analysis reveals a very low energy distribution (Fig. 3); thus, the three new, recently found polymorphs (Lopez-Mejias et al., 2009) should not represent a surprise and possibility of further polymorphs cannot be ruled out. In fact, the torsion angles, τ_1, of the conformers in these crystals are -138.4° and 126.8° in form III ($Z' = 2$), -115.8°, -125.9°, and -134.1° in form IV ($Z' = 3$), and -125.1° in form V; the conformational energy difference among these conformers is again within a few kJ/mol (Fig. 3). That is supportive of the often quoted McCrone's argument that the number of forms discovered is up to the time and effort spent for them (McCrone, 1965).

4. Conclusions

The conformational polymorphism of TFA is likely caused by the energy competition between delocalization of intramolecular π systems and enforcement of intermolecular hydrogen-bonding. From an energetic standpoint, TFA molecule prefers to remain relatively flat so as to maximize the molecular stability. On the other hand, due to its flexibility and low conformational energy barrier, TFA molecule can assume a different conformation augmented by crystal growth conditions. As the solute concentration increases, the conformational re-arrangement is favored kinetically by the low energy barrier and is driven thermodynamically by formation of stronger hydrogen bonding upon dimerization. The impact of the conformational flexibility on modulating intermolecular interactions is ultimately reflected in its crystal structures. By addressing the molecular and mechanistic aspects underlying the interplay between molecular conformation and intermolecular interaction, DFT concepts can yield considerable insight into the polymorphic behaviors of this system and, likely, many more to be investigated.

Acknowledgements

The authors acknowledge the Institute for High Performance Computing and the Center for Computational Sciences, University of Kentucky, for providing the computer resources. The study was supported by NSF (DMR-0449633 and DMR-1006364).

References

Addadi, L., Berkovitch-Yellin, Z., Weissbuch, I., van Mill, J., Shimon, L.J.W., Lahav, M., Leiserowitz, L., 1985. Growth and dissolution of organic crystals with "tailor-madeïnhibitors—implications in stereochemistry and materials science. Angew. Chem. Int. Ed. Engl. 24, 466–485.

Amovilli, C., Barone, V., Cammi, R., Cances, E., Cossi, M., Mennucci, B., Pomelli, C.S., Tomasi, J., 1999. Recent advances in the description of solvent effects with the polarizable continuum model. In: Adv. Quantum Chem., vol. 32: Quantum Systems in Chemistry and Physics, Pt II. Academic Press Inc., San Diego, pp. 227–261.

Andersen, K.V., Larsen, S., Alhede, B., Gelting, N., Buchardt, O., 1989. Characterization of 2 polymorphic forms of tolfenamic acid, N-(2-methyl-3-chlorophenyl)anthranilic acid—their crystal structures and relative stabilities. J. Chem. Soc. Perkin Trans. 2, 1443–1447.

Aubrey-Medendorp, C., Swadley, M.J., Li, T., 2008. The polymorphism of indomethacin: an analysis by density functional theory calculations. Pharm. Res. 25, 953–959.

Ayers, P.W., 2007. The physical basis of the hard/soft acid/base principle. Faraday Discuss. 135, 161–190.

Ayers, P.W., 2008. The dependence on and continuity of the energy and other molecular properties with respect to the number of electrons. J. Math. Chem. 43, 285–303.

Ayers, P.W., Levy, M., 2000. Perspective on "density functional approach to the frontier-electron theory of chemical reactivity". Theor. Chem. Acc. 103, 353–360.

Ayers, P.W., Morell, C., De Proft, F., Geerlings, P., 2007. Understanding the Woodward–Hoffmann rules by using changes in electron density. Chem. Eur. J. 13, 8240–8247.

Ayers, P.W., Morrison, R.C., Roy, R.K., 2002. Variational principles for describing chemical reactions: condensed reactivity indices. J. Chem. Phys. 116, 8731–8744.

Barone, V., Cossi, M., Tomasi, J., 1997. A new definition of cavities for the computation of solvation free energies by the polarizable continuum model. J. Chem. Phys. 107, 3210–3221.

Becke, A.D., 1988. Density-functional exchange-energy approximation with correct asymptotic behavior. Phys. Rev. A 38, 3098–3100.

Boys, S.F., Bernardi, F., 1970. Calculation of small molecular interactions by differences of separate total energies—some procedures with reduced errors. Mol. Phys. 19, 553–566.

Brittain, H.G., 2009. Polymorphism in Pharmaceutical Solids. Informa Healthcare USA, Inc., New York, NY.

Byrn, S.R., Pfeiffer, R.R., Stowell, J.G., 1999. Solid State Chemistry of Drugs, second ed. SSCI, Inc., West Lafayette, IN.

Cardenas, C., Rabi, N., Ayers, P.W., Morell, C., Jaramillo, P., Fuentealba, P., 2009. Chemical reactivity descriptors for ambiphilic reagents: dual descriptor, local hypersoftness, and electrostatic potential. J. Phys. Chem. A 113, 8660–8667.

Davey, R.J., Blagden, N., Potts, G.D., Docherty, R., 1997. Polymorphism in molecular crystals: stabilization of a metastable form by conformational mimicry. J. Am. Chem. Soc. 119, 1767–1772.

Dennington, R., Keith, T., Millam, J., Eppinnett, K., Hovell, W.L., Gilliland, R., 2003. GaussView Version 4.0. Semichem, Inc., Shawnee Mission, KS.

Desiraju, G.R., 2007. Crystal engineering: a holistic view. Angew. Chem. Int. Ed. Engl. 46, 8342–8356.

Dobson, J.F., McLennan, K., Rubio, A., Wang, J., Gould, T., Le, H.M., Dinte, B.P., 2001. Prediction of dispersion forces: is there a problem? Aust. J. Chem. 54, 513–527.

Dunitz, J.D., Gavezzotti, A., 2009. How molecules stick together in organic crystals: weak intermolecular interactions. Chem. Soc. Rev. 38, 2622–2633.

Etter, M.C., 1990. Encoding and decoding hydrogen-bond patterns of organic compounds. Acc. Chem. Res. 23, 120–126.

Feng, X.T., Yu, J.G., Lei, M., Fang, W.H., Liu, S.B., 2009. Toward understanding metal-binding specificity of porphyrin: a conceptual density functional theory study. J. Phys. Chem. B 113, 13381–13389.

Frenking, G., Frohlich, N., 2000. The nature of the bonding in transition-metal compounds. Chem. Rev. 100, 717–774.

Frisch, M.J., Trucks, G.W., Schlegel, H.B., Scuseria, G.E., Robb, M.A., Cheeseman, J.R., Montgomery, J.A., Vreven, T., Kudin, K.N., Burant, J.C., Millam, J.M., Iyengar, S.S., Tomasi, J., Barone, V., Mennucci, B., Cossi, M., Scalmani, G., Rega, N., Petersson, G.A., Nakatsuji, H., Hada, M., Ehara, M., Toyota, K., Fukuda, R., Hasegawa, J., Ishida, M., Nakajima, T., Honda, Y., Kitao, O., Nakai, H., Klene, M., Li, X., Knox, J.E., Hratchian, H.P., Cross, J.B., Bakken, V., Adamo, C., Jaramillo, J., Gomperts, R., Stratmann, R.E., Yazyev, O., Austin, A.J., Cammi, R., Pomelli, C., Ochterski, J.W., Ayala, P.Y., Morokuma, K., Voth, G.A., Salavdor, P., Dannenberg, J.J., Zakrzewski, V.G., Dapprich, S., Daniels, A.D., Strain, M.C., Farkas, O., Malick, D.K., Rabuck, A.D., Raghavachari, K., Foresman, J.B., Ortiz, J.V., Cui, Q., Baboul, A.G., Clifford, S., Cioslowski, J., Stefanov, J.B., Liu, G., Liashenko, A., Piskorz, P., Komaroni, I., Martin, R.L., Fox, D.J., Keith, T., Al-Laham, A., Peng, C.Y., Nanayakkara, A., Challacombe, M., Gill, P.M.W., Johnson, B., Chen, W., Wong, M.W., Gonzalez, C., Pople, J.A., 2004. Gaussian 03 Revision C.02. Gaussian, Inc., Wallingford, CT.

Geerlings, P., De Proft, F., Langenaeker, W., 2003. Conceptual density functional theory. Chem. Rev. 103, 1793–1873.

Hollingsworth, M.D., 2002. Crystal engineering: from structure to function. Science 295, 2410–2413.

Huang, Y., Zhong, A., Rong, C., Xiao, X., Liu, S.B., 2008. Structure, spectroscopy, and reactivity properties of porphyrin pincers: a conceptual density functional theory and time-dependent density functional theory study. J. Phys. Chem. A 112, 305–311.

Kohn, W., Meir, Y., Makarov, D.E., 1998. van der Waals energies in density functional theory. Phys. Rev. Lett. 80, 4153–4156.

Lee, E.H., Boerrigter, S.X.M., Rumondor, A.C.F., Chamarthy, S.P., Byrn, S.R., 2008. Formation and solid-state characterization of a salt-induced metastable polymorph of flufenamic acid. Cryst. Growth Des. 8, 91–97.

Li, T., 2007. Understanding the polymorphism of aspirin with electronic calculations. J. Pharm. Sci. 96, 755–760.
Li, T., Ayers, P.W., Liu, S.B., Swadley, M.J., Aubrey-Medendorp, C., 2009. Crystallization force—a density functional theory concept for revealing intermolecular interactions and molecular packing in organic crystals. Chem. Eur. J. 15, 361–371.
Long, S., Li, T., 2009. Controlled formation of the acid-pyridine heterosynthon over the acid–acid homosynthon in 2-anilinonicotinic acids. Cryst. Growth Des. 9, 4993–4997.
Long, S., Parkin, S., Siegler, M.A., Cammers, A., Li, T., 2008. Polymorphism and phase behaviors of 2-(phenylamino)nicotinic acid. Cryst. Growth Des. 8, 4006–4013.
Lopez-Mejias, V., Kampf, J.W., Matzger, A.J., 2009. Polymer-induced heteronucleation of tolfenamic acid: structural investigation of a pentamorph. J. Am. Chem. Soc. 131, 4554–4555.
McCrone, W.C., 1965. Polymorphism. In: Labes, D., Weissberger, M.M.A. (Eds.), Physics and Chemistry of the Organic Solid Fox. Interscience Publishers, New York, pp. 725–767.
Morell, C., Grand, A., Toro-Labbe, A., 2005. New dual descriptor for chemical reactivity. J. Phys. Chem. A 109, 205–212.
Nangia, A., 2008. Conformational polymorphism in organic crystals. Acc. Chem. Res. 41, 595–604.
Parmar, M.M., Khan, O., Seton, L., Ford, J.L., 2007. Polymorph selection with morphology control using solvents. Cryst. Growth Des. 7, 1635–1642.
Parr, R.G., Von Szentpaly, L., Liu, S.B., 1999. Electrophilicity index. J. Am. Chem. Soc. 121, 1922–1924.
Parr, R.G., Yang, W.T., 1984. Density functional approach to the Frontier-electron theory of chemical reactivity. J. Am. Chem. Soc. 106, 4049–4050.
Parr, R.G., Yang, W.T., 1989. Density Functional Theory of Atoms and Molecules. Oxford University Press, New York.
Perdew, J.P., Parr, R.G., Levy, M., Balduz, J.L., 1982. Density functional theory for fractional particle number: derivative discontinuities of the energy. Phys. Rev. Lett. 49, 1691–1694.
Price, S.L., 2009. Computed crystal energy landscapes for understanding and predicting organic crystal structures and polymorphism. Acc. Chem. Res. 42, 117–126.
Reed, A.E., Curtiss, L.A., Weinhold, F., 1988. Intermolecular interactions from a natural bond orbital, donor–acceptor viewpoint. Chem. Rev. 88, 899–926.
Reed, A.E., Weinhold, F., 1983. Natural bond orbital analysis of near-Hartree–Fock water dimer. J. Chem. Phys. 78, 4066–4073.
Roy, D.R., Chattaraj, P.K., 2008. Reactivity, selectivity, and aromaticity of Be-3(2-) and its complexes. J. Phys. Chem. A 112, 1612–1621.
Steiner, T., 2002. The hydrogen bond in the solid state. Angew. Chem. Int. Ed. Engl. 41, 48–76.
Threlfall, T., 2000. Crystallisation of polymorphs: thermodynamic insight into the role of solvent. Org. Process Res. Dev. 4, 384–390.
Ugur, I., De Vleeschouwer, F., Tuzun, N., Aviyente, V., Geerlings, P., Liu, S.B., Ayers, P.W., De Proft, F., 2009. Cyclopolymerization reactions of diallyl monomers: exploring electronic and steric effects using DFT reactivity indices. J. Phys. Chem. A 113, 8704–8711.
Weissbuch, I., Lahav, M., Leiserowitz, L., 2003. Toward stereochemical control, monitoring, and understanding of crystal nucleation. Cryst. Growth Des. 3, 125–150.
Yang, W., Mortier, W.J., 1986. The use of global and local molecular parameters for the analysis of the gas-phase basicity of amines. J. Am. Chem. Soc. 108, 5708–5711.
Yang, W.T., Parr, R.G., 1985. Hardness, softness, and the Fukui function in the electronic theory of metals and catalysis. Proc. Natl. Acad. Sci. U.S.A. 82, 6723–6726.
Yu, L., 2010. Polymorphism in molecular solids: an extraordinary system of red, orange, and yellow crystals. Acc. Chem. Res. 43, 1257–1266.